ORIGIN & GENESIS OF CALCRETE IN THE MURRAY BASIN

L.N. Tylkowski

Supervisors D.J. Chittleborough & K.M. Barovich

Cooperative Research Centre for Landscape Evolution and Mineral Exploration (CRC LEME)
School of Earth and Environmental Sciences, University of Adelaide, Adelaide SA 5005, Australia
luke.tylkowski@adelaide.edu.au

ORIGIN & GENESIS OF CALCRETE IN THE MURRAY BASIN

L.N. Tylkowski

Supervisors D.J. Chittleborough & K.M. Barovich

.

Cooperative Research Centre for Landscape Evolution and Mineral Exploration (CRC LEME)
School of Earth and Environmental Sciences, University of Adelaide, Adelaide SA 5005, Australia
luke.tylkowski@student.adelaide.edu.au

FIGURES

TABLES

ABSTRACT

Calcretes and other terrestrial carbonate accumulations have formed throughout the Murray Basin during the Quaternary, particularly in far western regions. Ooids and grain coatings of $CaCO_3$ by infiltrating carbonate saturated solutions indicate calcrete has formed through pedogenic processes. Based on different morphologies and spatial relationships calcretes historically have been identified as either the younger Bakara or older Ripon Calcrete. The congruence of different stratigraphic calcretes, particularly the Bakara and Ripon Calcretes, was shown by clay mineralogy and the ratio of immobile elements. Three distinct sedimentological units were differentiated through zircon/rutile ratios of the heavy mineral fraction (>2.9 g/cm^3); the underlying Blanchetown Clay and two differing aeolian units including the Woorinen Formation. The strontium isotope signature in all of the calcretes and carbonate material in the profile is believed to be due to an aeolian source from a marine environment. A model of calcrete development was constructed that incorporated illuviation of carbonate saturated solutions and other pedogenic processes synchronous with an aeolian deposition of highly calcareous material.

KEY WORDS: calcrete, carbonate, pedogenesis, sedimentary, Pleistocene, resistant, strontium

INTRODUCTION

The term "calcrete" was applied by Lamplugh (1902) to Pleistocene gravels cemented by lime in the Bay of Dublin. Netterberg (1969) refined the term and applied it to "terrestrial material that had been cemented and/or replaced dominantly by $CaCO_3$...cave deposits excluded….". Calcrete herein describes indurated horizons cemented predominantly by $CaCO_3$. Non-indurated horizons with high percentages of $CaCO_3$ (>20 wt %) are described as carbonate layers.

The formation of calcrete has been attributed to the following processes; pedogenic (Gile *et al*. 1966; Khadkikar *et al*. 2000; Arakel 1995), rhizomorphic (Klappa 1980a; Klappa 1980b; Calvet & Julia 1983), physiochemical and groundwater (Khadkikar *et al*. 2000). The distinction between these processes is unclear as similar morphologies of calcrete can arise from different processes. However, many studies of calcrete genesis have been formulated (e.g. Kahle 1977; Beier 1987; Wright *et al*. 1988). Additionally, those of Gile *et al*. (1966), Netterberg (1967) and Arakel (1995) have proposed models of calcrete formation.

The genesis of calcretes in the Cainozoic Murray Basin, southern Australia, is a matter of much speculation. Calcrete formation is common throughout the Murray Basin, although in the southwestern region calcrete is typically in the form of massive sheets (Brown & Stephenson 1991). Elsewhere to the east and north, underlying aeolian sands, calcretes are rubbly and less indurated (Brown & Stephenson 1991). Firman (1964, 1967) and others (Wetherby & Oades 1975) have assigned various carbonate layers to particular stratigraphic units based on morphology. Nodular calcrete that is contained in siliceous soil is referred to as Bakara Calcrete to which they have assigned a younger stratigraphic age than the underlying pink, heavily indurated layer called Ripon Calcrete. These workers have not given consideration that *in-situ* processes may have generated the various carbonate morphologies, and in turn, implicate that the Bakara and Ripon Calcretes have formed in the one calcareous deposit; i.e. they are not separate stratigraphic units.

The source of Ca for pedogenic carbonates includes parent material (Boettinger & Southard 1991), surface and groundwater (Watts 1980; Arakel 1982), airborne dust and ash (Gile *et al*. 1966; Hay & Reeder 1978; Klappa 1980a; Warren 1983), precipitation (Gardner 1972) and seawater (Kahle 1977). Calcium in a majority of calcretes studied near coastal areas is considered to have originated from sea spray or airborne dust (see aforementioned references).

Groundwater sources are localised in areas of high water tables and on the flanks of rivers (Arakel 1982). Parent materials that have weathered from rocks and sediments high in Ca, such as basalts and limestones, can also be a source (Milnes & Ludbrook 1986). Within the Murray Basin an aeolian source of Ca is widely accepted, although untested by new tracer techniques. In many areas it is referred to as Crocker's Loess (Crocker 1946)

A technique that can distinguish the source of Ca in calcretes is strontium isotope analysis, as Sr is a proxy for Ca based on ionic radius and charge. Several studies using $^{87}Sr/^{86}Sr$ ratios have concluded that aeolian/atmospheric deposition of Ca is the main process in the formation of pedogenic carbonates (Van der Hoven & Quade 2002; Yang *et al*. 2000; Hamidi *et al*. 2001; Chiquet *et al*. 1999). Nevertheless, other studies have concluded that leaching of Ca from the parent material is the major source (Capo *et al*. 2000).

The aim of this project is to investigate the genesis of calcrete, in particular the Bakara and Ripon calcretes, to determine the difference or similarity between the origins of these carbonate morphologies. Specifically we test the hypothesis that weathering and translocation processes are responsible for the morphologies of these widespread types in the Murray Basin. The criteria we use include particle size distributions, very fine sand (VFS) to fine sand (FS) ratios, heavy mineral ratios and Sr isotope analysis as well as clay mineralogy, carbonate concentration and thin section petrology. Strontium isotope analysis can test the hypothesis that the source of Ca in calcretes within the Murray Basin is from the weathering of underlying material.

GEOLOGICAL SETTING & PROFILE STRATIGRAPHY

The Murray Basin is a shallow intracratonic sedimentary basin composed of a Cainozoic sedimentary succession that reaches a maximum thickness of 600 m in the central region (Figure 1) (Brown & Stephenson 1991). The separation of Antarctica and the southern margin of Australia during the Late-Mesozoic-Early Cainozoic (Cande & Mutter 1982) initiated sedimentation. Although subtle tectonic movements have impacted on sedimentation the dominant factor has been eustacy, particularly elevated sea levels (Brown & Stephenson 1991).

Tertiary sedimentation can be divided into three depositional periods separated by mid and late Tertiary hiatuses (Brown & Stephenson 1991); 1) Paleocene to Lower Oligocene sedimentation dominated by the Renmark Group, composed of sands, silts and clays; 2) Oligocene to middle Miocene deposition of the Murray Group (mainly limestones) in the western portion and Geera Clay and Winnambool Formation in the east; 3) Upper Miocene to Pliocene sequence of mainly Loxton-Parilla Sands, lacustrine Bookpurnong Beds in the western portion and silts/sands of the Shepparton and Calvil formations in the east (Figure 1).

At the base of the Sedan profile (Figure 2) is the Pliocene to late Pleistocene Blanchetown Clay (Stephenson 1986), or an equivalent sediment. The unit is a red-brown, silty clay that has strong ped development. The thickness of the unit is unknown. The unit was deposited under fluvial-lacustrine conditions in an extensive terrestrial body called Lake Bungunnia (Firman 1965, 1973; Stephenson 1986). This lake was formed by tectonic damming of the Murray River, further east of Sedan, at approximately 2.5 Ma. The lake was restricted east of Sedan by the Morgan Fault; hence, the studied profile is situated outside the proposed area of Lake Bungunnia.

Situated above the Blanchetown Clay is a mottled transitional horizon that contains powdery carbonate within the clay unit (Figure 2). This horizon marks the beginning of a series of strongly calcareous horizons wherein the top units conform to pre-existing stratigraphy that was outlined by Firman (1964, 1967, 1972, 1973). The age of these calcareous horizons is based on stratigraphic relationships as they overlie the Blanchetown Clay (plus equivalents) and Bridgewater Formation and underlie the Woorinen Formation (Firman 1967). By this rationale an age of Early Pleistocene to Holocene (Firman 1967) is established, considering calcrete formation overprints existing geological materials as a carbonate precipitate.

Following 0.5 m horizon of undifferentiated carbonate a 17 cm section of Ripon calcrete is present (Figure 2). Firman (1973) asserted that this calcrete is older than the overlying Bakara Calcrete. The highly indurated, pink Ripon Calcrete contains various intraclasts and multiple carbonate concretions (Firman 1973). The younger Bakara Soil contains nodular calcrete within an organic-rich sandy soil (Figure 2). The genesis of these calcretes is believed to be the result of a pedogenic process that occurred during the late Quaternary. However, groundwater activity and lateral movement of Ca is a process that may have a bearing on the formation of calcrete (Arakel 1982). Wetherby & Oades (1975) studied calcretes within the Woorinen Formation and concluded a more humid climate with inactive and vegetated dunes produced favourable conditions for the precipitation of pedogenic calcrete.

The material overlying the Bakara Calcrete is a dark brown sand (Woorinen Formation) from the Late Pleistocene with possible Holocene remobilisation (Brown & Stephenson 1991). Regionally this unit appears east of the Tertiary Murray units with a large aerial distribution (Figure 1). This unit has experienced pedogenesis with sandy and silty sediments being mixed with clay aggregates and humic material (leaf litter, twigs and rootlets) (Brown & Stephenson 1991). This is consistent with eluvial processes characteristic of an A horizon; nevertheless, the unit may have formed by aeolian deposition and been subjected to minor in-situ pedogenesis. Brown & Stephenson (1991) have proposed the coalescence of nodular calcrete at the base of the Woorinen Formation that can be considered part of the Qca unit (see Figure 1).

METHODS

Field sampling

Despite extensive Tertiary sedimentation, the profile selected near Sedan, South Australia (Figure 1), has predominantly Quaternary units represented. The profile is situated in the far western portion of the Murray Basin within the Mid-Murray Shire of rural South Australia. Locally it is 5 km east of the township of Sedan along the Sedan-Swan Reach Road at the co-ordinates of 0348928/6173051 (GDA 94-Zone 54). This particular site was chosen as it has a large thickness (approximately 1 m) of differing morphologies of calcrete including nodular (Bakara Calcrete), indurated (including Ripon Calcrete), laminated and powdery forms.

The initial step of the sampling procedure was to cut back approximately 30 cm horizontally from the profile face to reduce anthropogenic effects from the nearby roadway. Two different types of samples were collected systematically from the profile. Representative bulk samples (Figure 2-1-9) (2-4 kg) were collected from the various horizons and placed in plastic bags. These samples were used for mineralogical, chemical and physical analysis (Figure 3). Undisturbed samples (Figure 2-Sx) were taken at depths reflecting differing regolith materials and morphologies. These samples were either used in density measurements or impregnated for petrographic analyses (Figure 3). All samples were cut out by knife and/or chisel with bulk samples aided by a shovel.

Chemical analysis

Dry soil was passed through a 2 mm sieve and the carbonate content of the >2 mm (gravel) and ≤2 mm (fine earth) fractions were measured by calcimetry described by Rayment & Higginson (1992). Approximately 0.05-0.1 g of sample was reacted with 20 ml of 4 M $HCl/FeCl_2$ solution. Organic carbon was measured by the method of Allison (1965) in which 1-4 g of soil was titrated with 10 ml of 1 N potassium dichromate solution ($K_2Cr_2O_7$) (reagents listed in Appendix 1).

Physical analysis

Bulk density measurements in triplicate were undertaken by the paraffin wax method of Blake & Hartage (1986). Drying of bulk samples (clods or peds) from each horizon at 105^0 C, with the exception of the Woorinen Formation, preceded the application of wax.

A particle-size separation was undertaken by passing the collected dried sample through a 2 mm round hole sieve to produce two fractions; gravel (>2 mm) and fine earth (≤2 mm). Except for the Blanchetown Clay, silicates and non-carbonate minerals were separated from the carbonate by acidification of 1-1.5 kg of sample in 1 M HCl. A combination of sieving and settling yielded five fractions: >2000-125 μm (coarse sand), 125-53 μm (fine sand), 53-20 μm (very fine sand), 20-2 μm (silt) and <2 μm (clay) (Gee & Or 2002) (Figure 3). Mineralogical analysis by field emission secondary electron microscopy (FESEM) and x-ray diffraction (XRD) were undertaken on selected fractions. After drying and weighing a 25 g sample was extracted, oxidised using a hydrogen peroxide solution (H_2O_2) to remove organic matter, centrifuged a number of times to remove any soluble salts and treated with the reagent calgon (10 mls) to aid in aqueous suspension of fine particles.

The 20-53 μm (very fine sand) and 53-125 μm (fine sand) fractions were selected to determine resistant heavy minerals, such as zircon and rutile, because they are commonly found in these fractions (Chittleborough 1991). In addition, minerals of this size are considered immobile with respect to vertical displacement (processes such as eluviation) and can aid in discriminating between pedological and sedimentological processes. Approximately 0.2 g of very fine sand and 0.5 g of fine sand were added to a saturated solution of sodium polytungstate, of density 2.9 g/cm^3. After centrifuging for 5 minutes at 3000 rpm the heavy mineral fraction was extracted by syphoning. Several washings were necessary to dilute the saturated reagent solution from the minerals, and after drying, a portion of sample was syringed onto filter paper and attached to a secondary electron microscope (SEM) stub.

Mineralogy

Carbon-coated samples were examined using a Philips XL30 field emission scanning electron microscope (FESEM). Field scans covered a majority of each stub at an accelerating voltage of 15 kV, 500x magnification and 10 second elemental count time. Fifteen elements (O, Mg, Al, Si, Y, P, Zr, Ti, Ca, La, Ce, Fe, W, Mn and K) were chosen to determine the composition and

mineralogy of the grains. For each scan elemental weight percentages (normalized to 100 %), position of the grain and dimensions of the grain were recorded.

Orientated clay (<2 μm) samples were prepared for mineralogical analysis by x-ray diffraction (XRD). A suspension of clay was pipetted onto filter paper, the exchange saturated with Mg by washing twice with $MgCl_2$, five times with deionized water and adding five drops of glycerol. The samples and membranes were fixed to 32 mm aluminium disks using double sided tape. XRD patterns were collected on a Philips PW1800 microprocessor-controlled diffractometer using Co Kα radiation, variable divergence slit and graphite monochromator. The diffraction patterns were recorded from 3 to 32° in steps of 0.05° 2 θ with a 2.0 second counting time per step.

Undisturbed soil samples were taken from the profile and six samples; two from the Blanchetown Clay (S1a212, S1a151), two from the undifferentiated carbonate layers (S3a107, S4a69), one from the Ripon Calcrete (S5a37) and one from the Bakara Calcrete (S6a26), were impregnated under a vacuum with an epoxy resin and cut into thin sections (approximately 25 μm thick). All thin sections were examined on a Nikon Optiphot2-Pol transmitted light optical microscope.

Strontium isotope analysis

Carbonate material from all horizons except the transition zone were analysed for their Sr isotopic composition by a method adapted from Naiman *et al*. (2000).

Approximately 100 mg of ground sample was reacted with 4 ml of 1 M acetic acid and left in an ultrasonic bath for an hour. Acetic acid dissolution separates the carbonates and the labile fraction (surface complexes on silicate minerals and interlayer cations of clays) from silicates (Naiman *et al*. 2000). Whole rock samples of the Blanchetown Clay were treated with concentrated HF, placed in sealed Teflon vials and left on a hotplate for four days. In preparation for ion exchange column extraction Sr complexes were converted to chlorides by the addition of HCl. Strontium isotopes were measured with a Finnigan MS 262 thermal ionisation mass spectrometer (TIMS) located at the University of Adelaide.

RESULTS

Field descriptions

All samples including bulk samples (1-9) and selected samples (s1-s5) are shown in Figure 2 at the appropriate depths. Figure 2 also contains a brief description and stratigraphic name of the various horizons according to known geology in the area (Thomson 1969; Firman 1972). The uppermost horizon or Woorinen Formation is a very fine grained siliceous horizon that has a dark brown colour due to the presence of organic matter. The underlying Bakara Soil contains 2-5 cm nodules in a medium to fine grain siliceous matrix with angular to subangular quartz. The matrix is a brown colour that contrasts the buff colour of the calcrete nodules and contains organic matter including rootlets. Underlying the Bakara Calcrete is a highly indurated calcrete often referred to as the Ripon Calcrete in South Australia. This unit is recognisable by its light pink colour and contains 1-2 cm laminations of calcrete at the top of the unit. Concretions of $CaCO_3$ are visible on inspection with some having quartz or other sand sized particles as the nucleus.

Below the Ripon calcrete is a 59 cm thick unnamed unit of indurated carbonate. It is of a lighter white colour to the above lying units, and at the base, has a mixture of indurated calcrete and powdery carbonate. Minor features include coarse quartz grains (some even ferruginized) with root hairs of 0.1-0.5 cm. Between the calcrete/carbonate layers and the Blanchetown Clay there is a 38 cm transition zone that is composed of segregations of carbonate within the Blanchetown Clay. The Blanchetown Clay itself has a distinctive red/brown colour with large peds (1-5 cm). This unit contains a large amount of clay and a black mineral that is believed to be birmessite (a manganese oxide commonly found in Pliestocene clays of the Murray Basin).

Chemical analyses

Organic matter and carbonate of both the fine earth and gravel fractions were measured chemically on all samples. The greatest values of organic matter in both the gravel (>2 mm) and fine earth fractions (≤2 mm) were in the uppermost horizons. In the Woorinen Formation, gravel and fine earth fractions have the same value (2.05 %), however in the underlying Bakara Calcrete there are higher levels of organic matter in the fine earth matrix (1.67 %) than in the nodular calcrete (0.46 %). The Ripon Calcrete (45.5 cm) and Bakara Calcrete (23.5 cm)

horizons have more than double the amount of organic matter compared with the underlying carbonate layers within the gravel fraction.

Carbonate content of the gravel fraction (70-82 %) was similar in the top 115 cm of the profile. This depth encompasses the Woorinen Formation, Bakara and Ripon Calcretes, carbonate layers and the uppermost section of the transitional horizon. The fine earth fraction of the Woorinen and Bakara Calcrete have similar carbonate percentages (12 and 19 % respectively) which are lower than the corresponding gravel fraction. The lower sample in the transition zone has a decreased carbonate percentage for both the gravel and fine earth fractions with respect to the carbonate/calcrete layers (57 % gravel and 40 % fine earth). The Blanchetown Clay is free of carbonate.

Physical properties

Bulk density decreases with depth for the calcrete and carbonate horizons (2.39-2.06 g/cm^3) with the Bakara and Ripon horizons being denser than the homogenised carbonate layers (Figure 4). The transition zone has a lower bulk density that is neither akin to the calcrete/carbonate horizons or the Blanchetown Clay.

There is a marked difference in the particle size distribution (PSD) (Figure 5b) between the calcareous layers and the Blanchetown Clay. The Blanchetown Clay has an elevated proportion of clay with respect to the calcretes, which are sand rich. The silt fraction remains relatively constant throughout the entire profile. The gravel (>2 mm) fraction and fine earth (≤2 mm) fractions have a similar PSD for all samples, thus, there is a similarity between the soil and nodular calcrete within the Woorinen Formation and Bakara Calcrete (Table 1).

The sand PSD shown as Figure 5c illustrates the consistency of the very fine sand (20-53 μm) and fine sand (53-125 μm) fractions throughout the length of the profile. An increase in the coarse sand fraction in the middle of the profile (within the carbonate layers) results in higher fine and very fine sand proportions in surrounding units. In a majority of samples an increase or decrease of the 20-53 μm fraction is replicated in the 53-125 μm fraction. The PSD of sand is similar between calcrete and soil within the Woorinen Formation and Bakara Calcrete.

The very fine sand to fine sand (VFS/FS) ratio is consistent in all calcrete/carbonate horizons and the Woorinen Formation in both the gravel and fine earth fractions with the exception of the

Woorinen Formation fine earth fraction. The transition zone also showed variation in the VFS/FS ratio, between the gravel and fine earth fractions, with the fine earth fraction being similar to the calcrete/carbonate horizons above. The Blanchetown Clay has an elevated VFS/FS ratio, distinct from all other units.

Mineralogy

HEAVY MINERALS

The heavy mineral composition of calcrete nodules and soil within the Woorinen Formation is presented in Table 2 (samples 9a and 9b). There are no major differences in mineralogy between samples of the 20-53 μm fraction. The 53-125 μm fraction has a distinct elevation in immobile elements (zircon, rutile) in the Blanchetown Clay relative to the calcrete/carbonate layers and Woorinen Formation (Table 2-sample 2b). The Blanchetown Clay has a three to four time increase in zircon, rutile and titanite with ilmenite more than double the concentration. Within the 53-125 μm fraction there is an overall increase in the proportion of heavy silicate minerals within the soil and calcrete horizons. The Blanchetown Clay is the only sample that has a comparable mineral assemblage between the 20-53 μm and 53-125 μm fractions.

CLAY

Clay composition from XRD illustrates the difference between calcareous horizons and the underlying Blanchetown Clay (Figure 8). Increased concentrations of smectite and randomly interstratified minerals are evident within the Blanchetown Clay as shown by the far left rise in Figure 8. Figure 8 furthermore shows a decrease in illite in the lower calcareous layers shown as the middle peak. Kaolinite is present within all samples and has a consistent relative intensity down the profile.

PETROGRAPHY

The Blanchetown Clay (Figure 9a, 9b) reveals a voskelsepic fabric i.e. a highly birefringent clay matrix in which there are particular concentrations of sand-sized clay around skeletal grains and voids. In particular, clays are often associated with channels, that are distinct from zones of predominantly sand and silt sized quartz grains of various morphologies. The second image from this sample (Figure 9b) shows the clay matrix coating quartz grains. The uppermost

section of the Blanchetown Clay has zones of carbonate which act as a matrix and often coat sand and silt grains, as shown by the dark crystalline material in Figure 9c. The carbonate matrix is surrounded by clay and forms both large (400 μm) and smaller (20 μm) spherical areas.

The lowest carbonate layer is dominated by a dense carbonate matrix that is unlaminated. Carbonate has infiltrated fractures within quartz grains (Figure 9d) and concentrates near void spaces (Figure 9e), between grains and along channels. The above lying sample (Figure 9f) has three distinct domains (1) void spaces, (2) carbonate-coated silicate grains or carbonate in a sparsely populated matrix and (3) dense carbonate matrix surrounding either silicate grains or existing carbonate zones. The Ripon Calcrete section shows many complex laminations of clay and carbonate at the top (Figure 9g) and carbonate coated grains throughout the sample. Under high magnification multiple fine laminations are composed of a densely compacted carbonate with quartz grains being present in some layers. A majority of the sample shows coated rounded grains surrounded by a dense carbonate matrix. Figure 9h reveals a large grain coated at least twice with carbonate and composed of coated quartz grains cemented together with carbonate. The Bakara Calcrete has a similar morphology, except that, dense laminations form in a circular pattern with zones of detrital siliceous sand and silt sized grains.

Strontium isotopes

The Sr isotope data (Figure 10) are from the carbonate/calcrete horizons and the Blanchetown Clay. The transition zone was omitted from the analysis because it has a mix of materials. The carbonate samples all have similar isotopic compositions despite varying in depth and morphology (Figure 10a 0.711). The Blanchetown Clay sample differs from the average carbonate value by being much greater (0.724).

DISCUSSION

Composition, mineralogy and chemistry

WOORINEN FORMATION

The Woorinen Formation, although labelled as a stratigraphic unit, has many attributes of an A horizon of a soil (e.g. high organic matter and a granular structure). There are appreciable amounts of smectite, illite and kaolinite and the silicate clay content is higher in the Woorinen Formation than in the underlying calcretes. This trend may reflect the original proportions of clay in the sedimentary material or that carbonate has been illuviated to form the calcrete horizons below the siliceous Woorinen Formation.

The difference between the amount of clay, silt and sand in the gravel and fine earth fractions in the Woorinen Formation is minimal (Table 1). Therefore it appears that the nodular calcrete that comprises a majority of the gravel fraction has formed *within* the surrounding fine earth fraction. The similarity between the fine sand fractions of the two fractions (gravel and fine earth) supports this hypothesis, however there is more very fine sand in the fine earth fraction. This may be due to the preference of calcite to coat and precipitate grains with a larger surface area, although this trend is not reflected in the underlying Bakara Calcrete. Another explanation is that the topsoil has been eroded and a sediment with a similar fine sand percentage with differing coarse and very fine sand distributions. Thus, the Woorinen Formation may be the result of two processes; in situ pedogenesis involving the loss of carbonate by leaching and subsequent erosion, and aggradation of fine quartz sand by aeolian processes.

CALCRETES AND CARBONATES

This section of the profile encompasses the Bakara and Ripon Calcretes plus the two carbonate layers. Compared to the Woorinen Formation organic matter is severely depleted in this calcareous section. Except for the fine earth fraction of the Bakara Calcrete, which has an organic carbon content similar to the fine earth fraction of the Woorinen Formation. Carbonate percentages of the gravel fractions for all calcrete/carbonate horizons are within typical values for calcretes (70-90 %-Goudie 1973). The amount of carbonate in the fine earth fractions is lower than the gravel fractions and is composed of more clay-sized phyllosilicates and silt to sand sized silicate grains.

The residual particle size distribution of the Bakara and Ripon calcretes is similar and it is concluded that these two units were formed in a similar sedimentary material and should not be differentiated stratigraphically as determined by Firman (1967). The ratio of VFS/FS is relatively constant throughout the calcrete/carbonate horizons despite marked differences in the absolute concentrations of these fractions. This may be due to the composition of the originally deposited sediment or the translocation of either very fine sand or fine sand down into the transition zone.

Smectite, which is often associated with calcretes (Khadkikar *et al*. 2000; Sancho *et al*. 1992), is present in appreciable amounts in the calcrete/carbonate layers. The homogeneous clay mineral assemblage in the calcrete/carbonate horizons has been attributed to translocation of clay due to leaching. The clay mineral assemblage is similar to calcretes occurring in the St Vincent Basin and other calcretes in South Australia (Phillips 1988).

TRANSITION ZONE

Two bulk samples were analysed from the transition zone, which has the appearance of segregations or zones of concentrations within the Blanchetown Clay. The percentage of carbonate in this zone is higher in the sample closer to the calcretes and lower in the sample closer to the Blanchetown Clay. There is a rapid depletion of carbonate with depth, probably an effect of the distribution of segregations or the uneven surface of the Blanchetown Clay prior to the deposition of aeolian material. Furthermore wetting and drying, shrink swell movements of the clay surface and bioturbidation all could have contributed to an uneven surface.

The VFS/FS ratio within the gravel fraction of this zone lies between the average carbonate and Blanchetown Clay values. A possible explanation is eluviation/illuviation processes of very fine sand fraction or weathering and alteration of the Blanchetown Clay prior to the deposition of aeolian material. Another hypothesis is that this horizon is a mixture of Blanchetown Clay and carbonate and reflects mixing of these aforementioned materials. The fine earth fraction shows similar ratios of VFS/FS to the powdery carbonate. This illustrates that the siliceous residual grains in this fraction are related to the overlying carbonate units.

Pedogenesis and genetic implications

Pedogenic calcrete formation can involve a number of differing processes including weathering, erosion, dissolution, precipitation, illuviation and sedimentary processes. Chemically resistant minerals such as zircon and rutile in the 20-53 μm and 53-125 μm fraction (large enough not to be subject to illuviation) are suitable for inferring genetic processes (Chittleborough 1991).

Three distinct sedimentary materials were distinguished by the zircon to rutile (Zr/Ru) ratio determined from the FESEM scans (Figure 7). The lowest ratio is assumed to be the Blanchetown Clay, the middle an aeolian carbonate deposit and the third another aeolian deposit. Morphology of calcrete does not correspond to the sedimentary material in which it formed, as the lower carbonate layer has a ratio closer to the Blanchetown Clay and the upper carbonate layer has a ratio closer to the presumed aeolian deposit. The FESEM scans were not conducted on all samples and analysis of samples from the transition zone would confirm whether there was cross-sedimentary imprinting of carbonate within the profile. The similarity in the Zr/Ru ratio between the Woorinen Formation fine earth and gravel fractions indicates that the nodular calcrete found in this horizon was formed within a differing sedimentary material to the underlying Bakara and Ripon Calcretes. There are at least two periods of calcrete genesis within the profile with a possible period of erosion and re-deposition of aeolian material. It is assumed the fine siliceous sand in the Woorinen Formation is derived from an aeolian source as nearby geomorphic units include lunettes, dunes and other aeolian features (Brown and Stephenson 1991).

Despite the zircon to rutile ratio possibly indicating two periods of pedogenic carbonate formation, the strontium isotope data shows consistency in the source of Ca for all carbonate/calcrete samples. This source material is believed to be aeolian sediment ultimately derived from a marine environment, as the average $^{87}Sr/^{86}Sr$ ratio of the carbonates (0.711) is only slightly greater than the Quaternary marine signature (0.709) (Burke *et al*. 1982). Another possible source is dissolved Ca in rainwater. Numerous researchers have concluded an aeolian marine source for Ca in the formation of calcrete in other areas (Chiquet *et al*. 1999; Yang *et al*. 2000; Van der Hoven & Quade 2002). Aeolian-derived calcium in pedogenic carbonates of coastal South Australia/Victoria has been demonstrated by Quade *et al*. (1995) who measured Sr isotope ratios of soil carbonate parallel to the prevailing wind vector. They suggested that Sr ratios may increase slightly inland reflecting diminishing proportions of marine aeolian Sr and a concomitant increase in terrestrial dust or bedrock.

Calcium contributions from the parent material are minimal, considering the dissimilar strontium isotope value (0.724) and the low percentage of carbonate in the Blanchetown Clay. An aeolian marine origin is supported by the prevailing wind direction being from the south-southwest (Quade *et al*. 1995). The southwesterly area of the Murray Basin in composed of a series of parallel dunes formed from aeolian material accumulating during glacial periods within the Quaternary (Figure 11-I) (Harvey *et al*. 2001). This may be the source of material which would therefore give a minimum age of calcrete development of approximately 0.8 Ma (conditional to the Blanchetown Clay having completed its deposition).

The Bakara and Ripon Calcretes and the upper carbonate layer are assumed to have formed within a material similar to the fine earth fraction of the Bakara Calcrete, despite not measuring the heavy mineral content of this sample. However, the particle size distribution shows a similar distribution of residual material between the gravel and fine earth of the calcretes and carbonate layers. This indicates the particle size distribution is not consistent with the genetic sedimentary layers derived from the FESEM scans. Petrological analysis of the carbonate samples showed numerous "dissolution and precipitation" features (Harwood 1988) of silicate crystals by $CaCO_3$ including pitted and corrugated edges of grains (Figure 9). This indicates that the carbonate saturated solution that precipitated $CaCO_3$ could have dissolved siliceous material, particularly of the clay and fine sand fractions. Dissolution of silicates in calcretes has been demonstrated by a number of authors (e.g. Hay & Reeder 1978; Watts 1980) and occurs due to the high pH (>10) (Multer & Hoffmeister 1968) infiltrating solutions. Thus, the various fractions would be homogenised between samples rich in carbonate and would not reflect the particle size distribution of the original sediment. The ratio of VFS/FS of the two samples from the transition zone indicates an increased percentage of fine sand within the gravel fraction, which has large peds of Blanchetown Clay, compared to the fine earth fraction that is dominated by carbonate. However, the ratio of fine sand to coarse sand (FS/CS) does not show the same trends as the VFS/FS ratio and is dictated by other pedogenic and/or sedimentary processes.

A consequence of the dissolution and/or translocation of detrital clay is that the petrographic identification of original sedimentary material is difficult. Clays are either dissolved by the infiltrating fluid or incorporated within the calcitic cement (Hay & Reeder 1978). Therefore, the separation of the Blanchetown Clay-aeolian sediment boundary was not evident within the carbonate/calcrete thin sections. Residual features such as coatings of clay on silicate grains and within grain fractures are present in all thin sections from the carbonate and calcrete

horizons. This process has been observed in other calcretes of varying morphologies (e.g. Hay & Reeder 1978). Coated clay is considered to be derived from illuviation processes and is not a residual feature of the sediment. This is reflected in the XRD analysis in so far as samples above the Blanchetown Clay have similar mineralogy's. However, residual clay coatings could be possible in carbonates derived from the Blanchetown Clay due to the presence of coatings in the parent material. Further petrographic analysis of the transition zone of moderate carbonate concentrations may indicate possible processes and residual features of the Blanchetown Clay in carbonate-cemented areas.

The petrographic, mineralogical and chemical similarity of differing calcretes and carbonates indicates that morphology is determined by another process not measured in this study. A number of authors (Multer & Hoffmeister 1968; Klappa 1980b; Beier 1987; Philips 1988; Khadkikar *et al*. 2000) have documented the role of organic matter in forming indurated terrestrial carbonates while others have related morphology to the level of profile maturity (Gile 1966; Netterberg 1967).

Within all carbonate and calcrete layers investigated by petrography there are areas of increased clay material that contain fine to medium grain silicates and an increased detrital component. This is either residual material from the original sediment or a concentration of material by the carbonate saturated fluid. Another feature common to all horizons are ooids and rims around detrital and non-detrital grains. The Bakara Calcrete contains multiple coatings indicating many periods of infiltrating carbonate fluids. Ooids and $CaCO_3$ coatings are a common feature of pedogenic calcretes (Hay & Reeder 1978; Calvet & Julia 1983; Khadkikar *et al*. 2000) and are often associated with other indurated carbonates (Harwood 1988). Ooids and rims are obvious macroscopically in the Bakara and Ripon Calcretes due to preferential coating of possibly birmessite (dark material) and iron complexes (red material) (Philips 1988). The distribution of $CaCO_3$-rich areas close to void spaces indicates the precipitation of $CaCO_3$ by infiltrating fluids that sequentially coated and infilled detrital sediment.

Calcrete development model

The following model is similar to a number of models of pedogenic carbonate development (Gile *et al*. 1966; Netterberg 1967) that involves illuviation of clay, leaching and precipitation of $CaCO_3$ in a soil profile. Netterberg (1967) proposed weathering, and possible erosion, before the precipitation of $CaCO_3$; a process not incorporated into the following model. It is uncertain whether the Blanchetown Clay was weathered prior to the deposition of the overlying aeolian material and subsequent carbonate leaching. Furthermore the maturity of the calcrete profile has not been linked to the morphologies present as proposed by Gile *et al*. (1966).

The model is based upon the deposition of aeolian material above the Blanchetown Clay (Figure 11-I) and either leaching and reprecipitation of $CaCO_3$ in the sediment or the leaching and precipitation of $CaCO_3$ by Ca, O_2 and CO_2 in the soil (McCauley & Roy 1974; Klappa 1980b). Precipitation occurs due to the evaporation of water and super saturation of $CaCO_3$ in the diminishing fluid (Wright *et al*. 1988). Clay particles are also illuviated and co-precipitated with $CaCO_3$ on grains as coatings or embedded within the matrix. Carbonate nodules and spherical ooids develop within the calcretes as well as powdery carbonate within the lower horizons (including the Blanchetown Clay). Induration of horizons occurs by $CaCO_3$ dominating the matrix, reducing the pore space and raising the bulk density, as shown by Goudie (1973). The highly siliceous top soil horizon is possibly eroded and a differing aeolian sediment is deposited (Woorinen horizon). Subsequent nodular calcrete formation has taken place within this horizon.

CONCLUSIONS

Despite morphological differences, the calcretes and carbonate layers within the profile have similar mineralogy, chemistry and residual particle size distributions. This may indicate a similar age for the calcretes, which would contradict the existing stratigraphy outlined by Firman (1967). Clay movement is synchronous with $CaCO_3$ precipitation, with all carbonate rich horizons exhibiting coated residual grains and similar clay mineralogy. Possibly three sedimentary materials were deposited within the studied section, the Blanchetown Clay and two differing aeolian deposits. At least two periods of calcrete formation have been identified which are not consistent with the defined sedimentary layers. The first period of carbonate deposition overprinted both the Blanchetown Clay and upper aeolian sediment. The second period of calcrete formation occurred within the Woorinen Formation with possibly remobilisation of the fine earth fraction. The source of Ca in all measured calcrete/carbonate horizons is a continental aeolian input (dust, rainwater, aerosols or a combination thereof) transported from a marine setting with minimal input from the underlying parent material. The particle size separation is not consistent with the sedimentary horizons differentiated by FESEM scans. However, the particle size distribution does show consistency between samples of high carbonate content which may be associated with weathering of silicate grains by high pH carbonate saturated fluids. Of the techniques implemented within this study none provided any links to calcrete morphology. Further studies integrating grain morphology, biological effects on calcrete formation and elemental analysis could identify different morphologies of calcrete in the Murray Basin.

ACKNOWLEDGEMENTS

I would like to thank CRC LEME and the University of Adelaide for providing funding and resources for my project. Both technical assistants David Bruce and Colin Rivers were instrumental in the analysis of samples accurately and efficiently. Thin sections were performed by Ian Pontifex and XRD analysis by Mike Raven (CSIRO). Scientific contributions were made by Lindsay Curtis, Steven Hill, Adrian Fabris, Andrew McCord and Robert Dart. Furthermore I wish to thank my colleagues Paul Wittwer and Liam McEntagart and dedicate this manuscript to Tony Capriuolo (R.I.P).

REFERENCES

ALLISON L.E. 1965 Organic Carbon *In*:. Black C.A. eds. *Methods of Soil Analysis, Part 1* pp. 1367-1378. America Society of Agronomy, Madison, USA.

ARAKEL A. V. 1982. Genesis of calcrete in Quaternary soil profiles, Hutt and Leeman lagoons, Western Australia. *Journal of Sedimentary Petrology* **52**, 109-125.

ARAKEL A. V. 1995. Quaternary vadose calcretes revisted. *AGSO Journal of Australian Geology and Geophysics* **16**, 223-229.

BEIER J. A. 1987. Petrographic and geochemical analysis of caliche profiles in a Bahamian Pleistocene dune. *Sedimentology* **34**, 991-998.

BLAKE G.R, HARTAGE K.H. 1986. Bulk Density *In*:. Klute A., & Page A.L. eds. *Methods of Soil Analysis Part 1-Physical Minealogical Methods* pp. 363-380. Soil Science Society of America, Madison, USA.

BOETTINGER J. L., SOUTHARD R. J. 1991. Silica and carbonate sources for Aridisols on a granitic pediment, western Mojave Desert. *Soil Science Society of America Journal* **55**, 1057-1067.

BROWN C. M., STEPHENSON A.E. 1991. *Geology of the Murray Basin, southeastern Australia*. Bureau of Mineral Resources, Geology and Geophysics Bulletin **235**

BURKE W. H., DENISON R. E., HETHERINGTON E. A., KOEPNICK R. B., NELSON H. F., OTTO J. B. 1982. Variation of seawater $^{87}Sr/^{86}Sr$ throughout Phanerozoic time. *Geology* **10**, 516-519.

CALVET F., JULIA R. 1983. Pisoids in the caliche profiles of Tarragona (NE Spain). *In*: Peryt Tadeusz, M. ed. *Coated grains,* pp. 456-473. Springer-Verlag, Berlin, Federal Republic of Germany.

CANDE S.C., MUTTER J.C.,1982. A revised identification of the oldest seafloor spreading anomalies between Australia and Antarctica. *Earth and Planetary Science Letters* **58**, 151-160

CAPO R.C., WHIPKEY C.E., BLACHERE J.E., CHADWICK O.A. 2000. Pedogenic origin of dolomite in a basaltic weathering profile, Kohala Peninsula, Hawaii. *Geology* **28**, 271-274.

CHIQUET A., MICHARD A., NAHON D., HAMELIN B. 1999. Atmospheric input vs in situ weathering in the genesis of calcretes; an Sr isotope study at Galvez (central Spain). *Geochimica et Cosmochimica Acta* **63**, 311-323.

CHITTLEBOROUGH D.J. 1991. Indices of weathering for soils and Palaeosols formed on silicate rocks. *Australian Journal of Earth Sciences* **38** 115-120

CROCKER R. L. 1946. *Post-Miocene climatic and geologic history and its significance in relation to the genesis of the major soil types of South Australia*. CSIRO (Commonwealth Scientific and Industrial Research Organization), Melbourne, Australia.

FIRMAN J.B. 1964. The Bakara Soil and other stratigraphic units of the Late Cainozoic age in the Murray Basin, South Australia. Geological Survey of South Australia*, Quaternary Geological Notes* **10**, 2-5

FIRMAN J.B. 1965. Late Cainozoic lacustrine deposits in the Murray Basin, South Australia. Geological Survey of South Australia, *Quaternary Geological Notes* **16**, 1-2

FIRMAN J.B. 1967. Stratigraphy of the Late Cainozoic deposits in South Australia. *Royal Society of South Australia Transactions* **91**, 165-177

FIRMAN J.B. 1972. Renmark map sheet. Geological Survey of South Australia, 1:250 000 Map Series.

FIRMAN J. B. 1973. *Regional stratigraphy of surficial deposits in the Murray Basin and Gambier Embayment*. Geological Survey of South Australia, Department of Mines and Energy, Adelaide, Australia.

GARDNER L. R. 1972. Origin of the Mormon Mesa Caliche, Clark County, Nevada. *Geological Society of America Bulletin* **83**, 143-155.

GEE G.W., OR D. 2002. Particle-size analysis *In*: Dawe J.H., & Topp G.C. eds. *Methods of Soil Analysis Part 4-Physical Methods* pp. 255-289. Soil Science Society of America, Madison, USA.

GILE L. H., PETERSON F. F., GROSSMAN R. B. 1966. Morphological and genetic sequences of carbonate accumulations in desert soils. *Soil Science* **101**, 347-360.

GOUDIE A. 1973. Duricrusts in tropical and subtropical landscapes. Clarendon Press, Oxford, United Kingdom.

HAMIDI E. M., COLIN F., MICHARD A., BOULANGE B., NAHON D. 2001. Isotopic tracers of the origin of Ca in a carbonate crust from the Middle Atlas, Morocco. *Chemical Geology* **176**, 93-104.

HARVEY N., BELPERIO A. P., BOURMAN R. P. 2001. Late Quaternary sea-levels, climate change and South Australian coastal geology. *In*: Gostin, V. A. ed. *Gondwana to greenhouse; Australian environmental geoscience,* pp. 201-215. Geological Society of Australia, Sydney, Australia.

HARWOOD G. M. 1988. Microscopic techniques; II, Principles of sedimentary petrography. *In*: Tucker, M. ed. *Techniques in sedimentology.*, pp. 108-173. Blackwell Science Publishing, Oxford, United Kingdom.

HAY R. L., REEDER R. J. 1978. Calretes of Olduvai Gorge and the Ndolanya Beds of northern Tanzania. *Sedimentology* **25**, 649-672.

KAHLE C. F. 1977. Origin of subaerial Holocene calcareous crusts; role of algae, fungi and sparmicritisation. *Sedimentology* **24**, 413-435.

KHADKIKAR A. S., CHAMYAL L. S., RAMESH R. 2000. The character and genesis of calcrete in late Quaternary alluvial deposits, Gujarat, western India, and its bearing on the interpretation of ancient climates. *Palaeogeography, Palaeoclimatology, Palaeoecology* **162**, 239-261.

KLAPPA C. F. 1980a. Brecciation textures and tepee structures in Quaternary calcrete (caliche) profiles from eastern Spain; the plant factor in their formation. *Geological Journal* **15**, 81-89.

KLAPPA C. F. 1980b. Rhizoliths in Terrestrial Carbonates - Classification, Recognition, Genesis and Significance. *Sedimentology* **27**, 613-629.

LAMPLUGH, G.W. 1902. Calcrete. *Geology Magazine* **9**, 575

McCAULEY J. W., ROY R. 1974. Controlled nucleation and crystal growth of various $CaCO_3$ phases by the silica gel technique. *American Mineralogist* **59**, 947-963.

MILNES A. R., LUDBROOK N. H. 1986. Provenance of microfossils in aeolian calcarenites and calcretes in southern South Australia. *Australian Journal of Earth Sciences* **33**, 145-159.

MULTER H. G., HOFFMEISTER J. E. 1968. Subaerial laminated crusts of the Florida Keys. *Geological Society of America Bulletin* **79**, 183-192.

NAIMAN Z., QUADE J., PATCHETT P. J. 2000. Isotopic evidence for eolian recycling of pedogenic carbonate and variations in carbonate dust sources throughout the Southwest United States. *Geochimica et Cosmochimica Acta* **64**, 3099-3109.

NETTERBERG F. 1967. Discussion on the nomenclature of soil carbonates. *Australian Journal of Science* **29**, 224-225.

NETTERBERG F. 1969. The interpretation of some basic calcrete types. *South African Archaeology Bulletin* **24**, 117-122.

PHILLIPS S.E. 1988. The interaction of geological, geomorphic and pedogenic processes in the genesis of calcrete. Phd thesis, University of Adelaide, Adelaide (unpub.)

QUADE J., CHIVAS A. R., McCULLOCH M. T. 1995. Strontium and carbon isotope tracers and the origins of soil carbonate in South Australia and Victoria. *Palaeogeography, Palaeoclimatology, Palaeoecology* **113**, 103-117.

RAYMENT, G.E., & HIGGSON, F.R. 1992. *Australian Laboratory Handbook of Soil and Water Chemical Methods*. Australian Soil and Land Survey Handbooks, 3, pp. 330. Inkata Press, Melbourne, Australia

SANCHO C., MELENDEZ A., SIGNES M., BASTIDA J. 1992. Chemical and mineralogical characteristics of Pleistocene caliche deposits from the central Ebro Basin, NE Spain. *Clay Minerals* **27**, 293-308.

STEPHENSON A. E. 1986. Lake Bungunnia; a Plio-Pleistocene megalake in southern Australia. *Palaeogeography, Palaeoclimatology, Palaeoecology* **57**, 137-156.

THOMSON B.P. 1969. *Adelaide 1:250 000 map sheet*. Geological Survey of South Australia, Department of Mines and Energy, Adelaide, Australia.

VAN DER HOVEN S. J., QUADE J. 2002. Tracing spatial and temporal variations in the sources of calcium in pedogenic carbonates in a semiarid environment. *Geoderma* **108**, 259-276.

WARREN J. K. 1983. Pedogenic calcrete as it occurs in Quaternary calcareous dunes in coastal South Australia. *Journal of Sedimentary Petrology* **53**, 787-796.

WATTS N. L. 1980. Quaternary Pedogenic Calcretes from the Kalahari (Southern-Africa) - Mineralogy, Genesis and Diagenesis. *Sedimentology* **27**, 661-686.

WETHERBY K.G., OADES J.M. 1975. Classification of carbonate layers in highland soils of the northern Murray Mallee, South Australia, and their use in stratigraphic and land use studies. *Australian Journal of Soil Research* **13**, 119-132

WRIGHT V. P., PLATT N. H., WIMBLEDON W. A. 1988. Biogenic laminar calcretes; evidence of calcified root-mat horizons in Paleosols. *Sedimentology* **35**, 603-620.

YANG J., CHEN J., AN Z., SHIELDS G., TAO X., ZHU H., JI J., CHEN Y. 2000. Variations in ($^{87}Sr/^{86}Sr$) ratios of calcites in Chinese loess: a proxy for chemical weathering associated with the East Asian summer monsoon. *Palaeogeography, Palaeoclimatology, Palaeoecology* **157**, 151-159.

Figure Captions

FIGURE 1

Cainozoic regional geological map of a western portion of the Murray Basin. Data contained within has been modified from State MGA GIS Dataset (PIRSA 2003-DVD ROM) and 1:250 000 map sheets (Thomson 1969; Firman 1972). Map co-ordinates are in Geodetics Datum of Australia (GDA) 94. Prescribed stratigraphic names are highlighted in bold font.

FIGURE 2

Sedan profile located 5km east of Sedan in rural South Australia (see Figure 1). All sample numbers are highlighted in bold with selected samples ranging from (**S6a26-S1c271**) and bulk samples ranging from (**9-1**) with increasing depth. Selected samples are categorised by stratigraphy as indicated by the initial numeral (**6-1**) and depth by the latter numeral (**23-271**). All depth values are in centimetres with the selected samples being represented at the proportional depth.

FIGURE 3

Flow chart of sequence of analyses. All boxes contain techniques implemented.

FIGURE 4

Carbonate percentage (%), organic matter (%) and bulk density of the fine earth (≤2mm) and gravel (>2mm) fractions of the Sedan profile (shown by photograph). All depths (in centimetres) and symbols are continuous from the carbonate (%) plot. Bulk density is presented in grams per cubic centimetre (g/cm^3). Carbonate (%) calculated from calcimetric measurement as per the methodology of Rayment and Higginson (1992). Organic matter (%) is a relative percentage and does not reflect actual percentages of organic matter in the soil (Allison 1965). Bulk density was determined from the paraffin wax method of Blake & Hartage (1986).

FIGURE 5

Particle size distribution (PSD) of the Sedan profile. (a) gravel (>2 mm) and fine earth (≤2 mm) fractions extracted by initial dry sieving, (b) percentage (%) sand, silt and clay of whole soil mass following removal of carbonate and aqueous suspension and (c) coarse sand (125-2000μm), fine sand (53-125 μm) and very fine sand (20-53 μm) of whole soil mass after carbonate removal and wet sieving. All depths are in centimetres (cm).

FIGURE 6

Very fine sand (VFS) to fine sand (FS) ratio of the gravel (>2 mm) and fine earth (≤2 mm), fractions of the Sedan profile. Dotted lines indicate stratigraphic boundaries between differing geological materials. VFS and FS were isolated by the particle size separation of the sand fraction. All depths are in centimetres (cm).

FIGURE 7

Zircon (Zr) to Rutile (Ru) ratio vs depth (centimetres) in the Sedan profile. Dotted lines indicate stratigraphic boundaries between differing geological materials. Symbols relate to proposed sedimentary material prior to calcrete development (⬡ Blanchetown Clay, ▲ Aeolian deposit A; and ▼ Aeolian deposit B). Actual percentages of zircon and rutile are presented in Table 1.

FIGURE 8

X-ray diffraction of relative intensity (y axis-counts per second) *vs* diffraction angle (x axis-2 theta degrees from a cobalt/potassium alpha source) of the clay fraction (<2 μm)

FIGURE 9

Thin section petrology of the Blanchetown Clay, carbonate and Ripon Calcrete horizons. (a) S1a212a-Clay particles are illustrated by the highly biofringent material and grey-black-white minerals are silicates. Channels of quartz and clay are stratified throughout the sample with clay being associated with void spaces. (b) S1a212b-Clay material infringing upon quartz grains. (c) S1a151-Upper Blanchetown Clay with infiltration of carbonate (dark brown material) as a matrix. (d) S1a107-Lower carbonate layer with inundation of carbonate to form spherical zones that have infiltrated quartz grains. (e) S1a107-Void spaces surrounded by a dense matrix of carbonate, differentiated from siliceous rich zones. (e) S1a69-Upper carbonate layer with three distinct areas from left to right; (1) void space, (2) carbonate coatings of grains in a sparsely populated matrix (3) dense carbonate matrix. (f) S1a37 Ripon Calcrete laminations with intermittent quartz grains. (g) S1a37-Carbonate infiltrated zone coated at least twice with carbonate illustrating multiple carbonate precipitation phases.

FIGURE 10

$^{87}Sr/^{86}Sr$ isotope data vs depth (centimetres). Reference $^{87}Sr/^{86}Sr$ isotopic values of seawater (Burke *et al*. 1992) and circles (●) represent carbonates and the square (■) the lower Blanchetown Clay horizon.

FIGURE 11

Genetic model of calcrete development in the Murray Basin. Symbols represent; (●) silicate minerals, (□) carbonate and (▬) clay. Aeolian deposition (I) of material from the Bridgewater Formation (calcareous dunes and calcrete) to Lake Bungunnia (Blanchetown Clay lacustrine source) during the Pleistocene. In-situ pedogenesis (II) by leaching of carbonate (pointed arrows) and illuviation of clay (dotted line). Carbonate accumulation and precipitation (III) by leaching and subsequent evaporation of carbonate saturated solutions. Present day profile (IV) (as shown in Figure 2) with the pointed arrows indicating a second aeolian deposition.

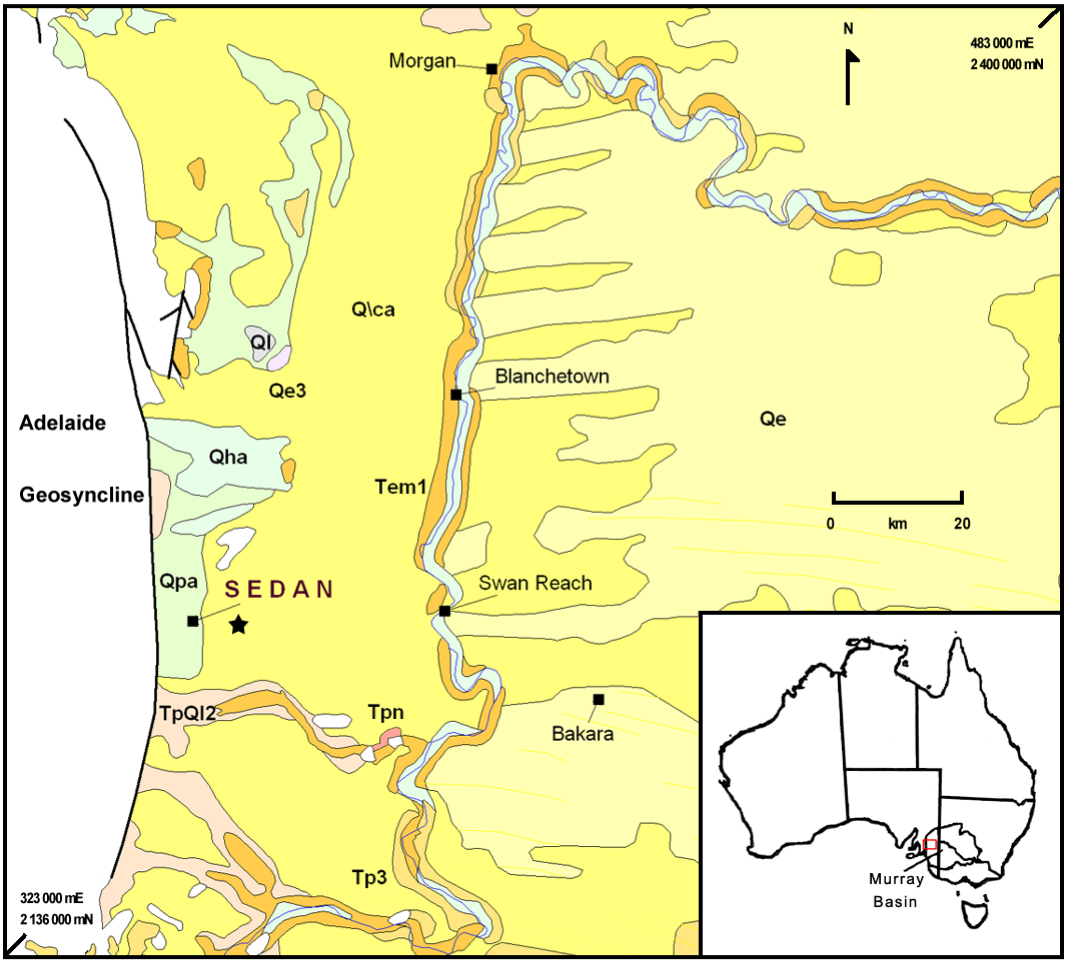

QUATERNARY

Ql	Undifferentiated playa/lacustrine sediments
Qha	Undifferentiated alluvial/fluvial sediments of the modern drainage channel
Qe3	Aeolian gypsiferous dune deposits, **Yamba Formation** equivalent
Qe	**Woorinen Formation** Aeolian quartz sand with carbonate silt and commonly contains nodular calcrete
Qpa	**Pooraka Formation** Alluvial/fluvial red brown sandy clay
Q\ca	Nodular calcrete in **Bakara Soil** and hardpan **Ripon Calcrete** below
TpQl2	**Blanchetown Clay & Bungunnia Limestone** Mottled sandy clay with clay matrix & fossiiferous dolomitic limestone

TERTIARY

Tpn	**Northwest Bend Formation** Estuarine oyster beds interbedded with quartz sands and calcareous sandstones
Tp3	**Parilla & Loxton Sands** Fluvial clay rich quartz sand and fluvio-lacustrine (Upper) & estuarine (Lower) micaceous sands
Tem1	**Morgan Limestone, Finniss Clay & Mannum Formation** Miocene fossiliferous marine lime-stone, clays & calcareous sandstone
	Pre Tertiary
	Fault
	Murray River
Morgan	Locality
★	Field Site

Sample No[0]	Depth	Description	Stratigraphy
9	0-10	Quartz rich loamy sand	Woorinen Formation
8 S6a23	10-37	Nodular calcrete	Bakara Calcrete
7 S5a37S5b37	37-54	Hardpan calcrete	Ripon Calcrete
6 S4a69 S3b97	54-89	Carbonate horizon	Carbonate Layer A
5 S3a107	89-113		Carbonate Layer B
4 S2b123	107-123	Clay rich horizon and powdery carbonate	Transition Zone
3	113-151		
S2a151			
2	151-175	Clay horizon with strong ped develop-ment and red/ yellow mottles	Blanche-town Clay
S1a212 S1b212			
1	175-234		
S1c271			

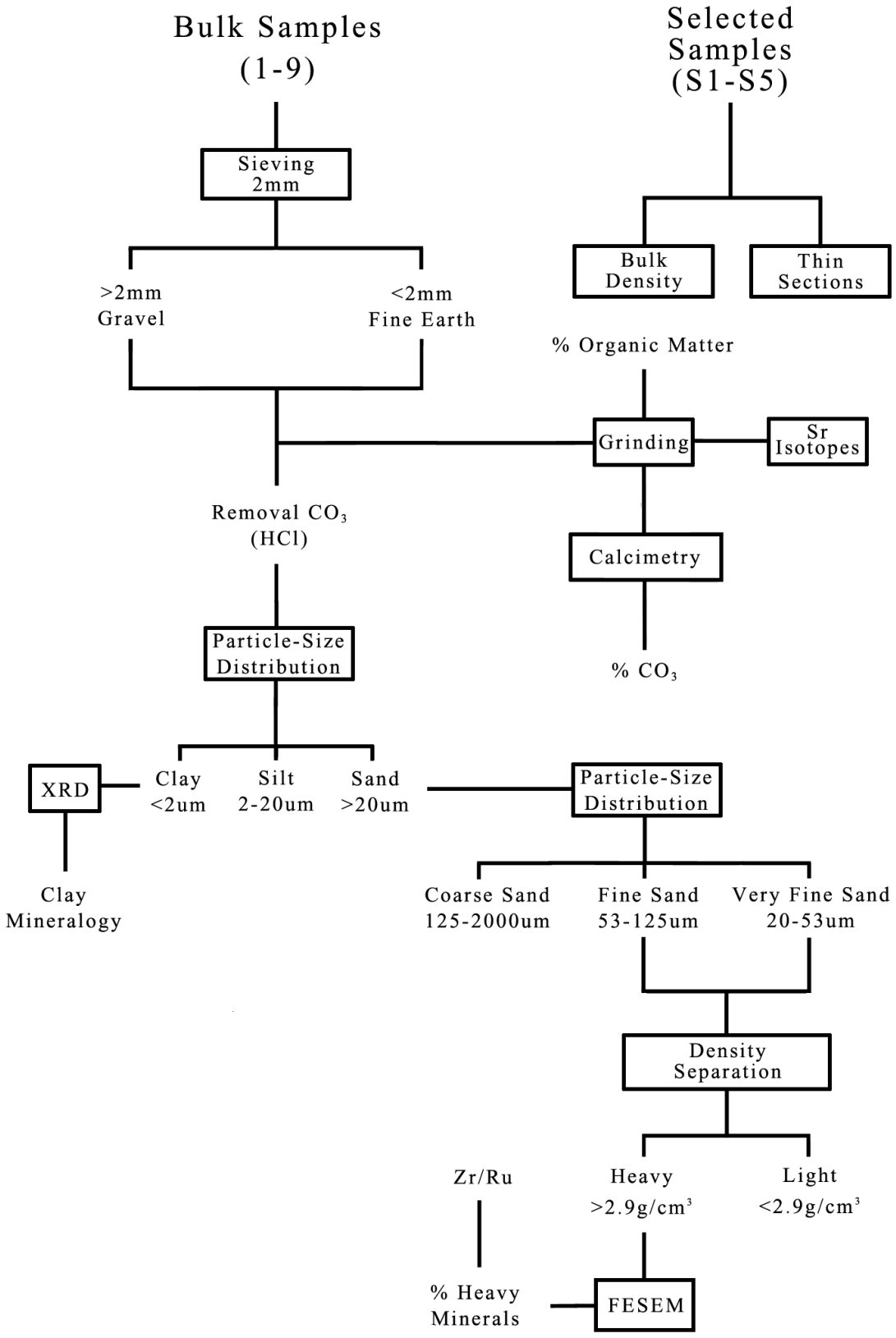
Bulk Samples
(1-9)
Selected
Samples
(S1-S5)
Sieving
2mm
>2mm
Gravel
<2mm
Fine Earth
Bulk
Density
Thin
Sections
% Organic Matter
Grinding
Sr
Isotopes
Removal CO_3
(HCl)
Calcimetry
Particle-Size
Distribution
% CO_3
XRD
Clay
<2um
Silt
2-20um
Sand
>20um
Particle-Size
Distribution
Clay
Mineralogy
Coarse Sand
125-2000um
Fine Sand
53-125um
Very Fine Sand
20-53um
Density
Separation
Zr/Ru
Heavy
>2.9g/cm³
Light
<2.9g/cm³
% Heavy
Minerals
FESEM

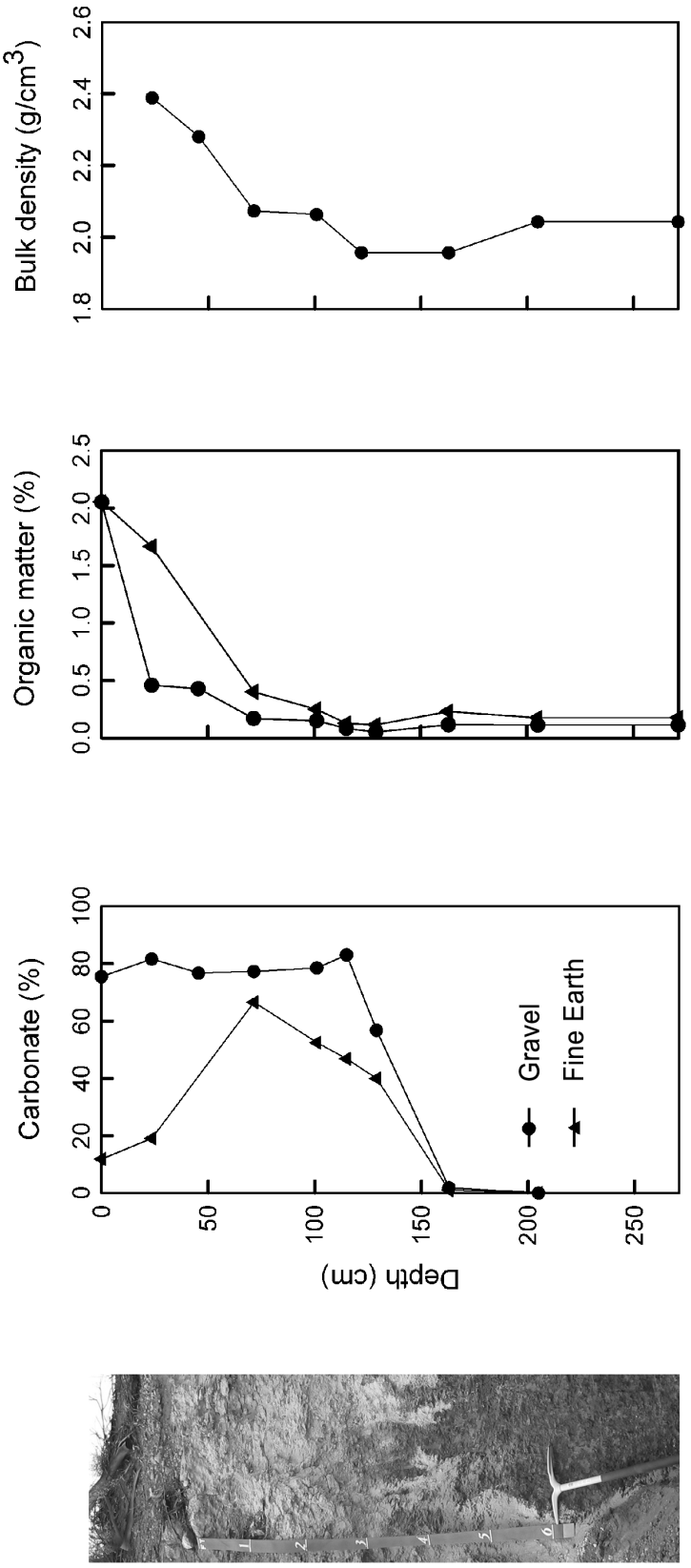
Bulk density (g/cm3)
1.8
2.0
2.2
2.4
2.6
Organic matter (%)
0.0
0.5
1.0
1.5
2.0
2.5
Carbonate (%)
0
20
40
60
80
100
Depth (cm)
0
50
100
150
200
250
Gravel
Fine Earth

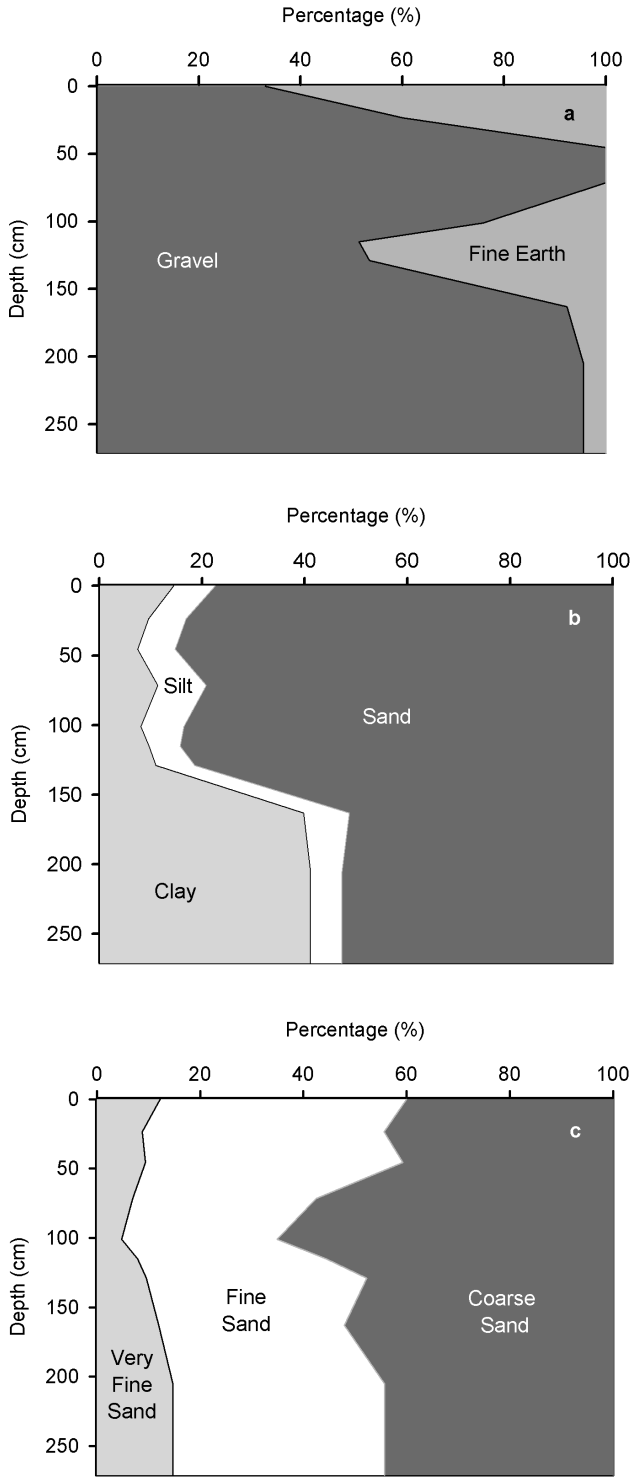
Percentage (%)
0
20
40
60
80
100
Depth (cm)
0
50
100
150
200
250
a
Gravel
Fine Earth
Percentage (%)
b
Silt
Sand
Clay
Percentage (%)
c
Fine
Sand
Coarse
Sand
Very
Fine
Sand

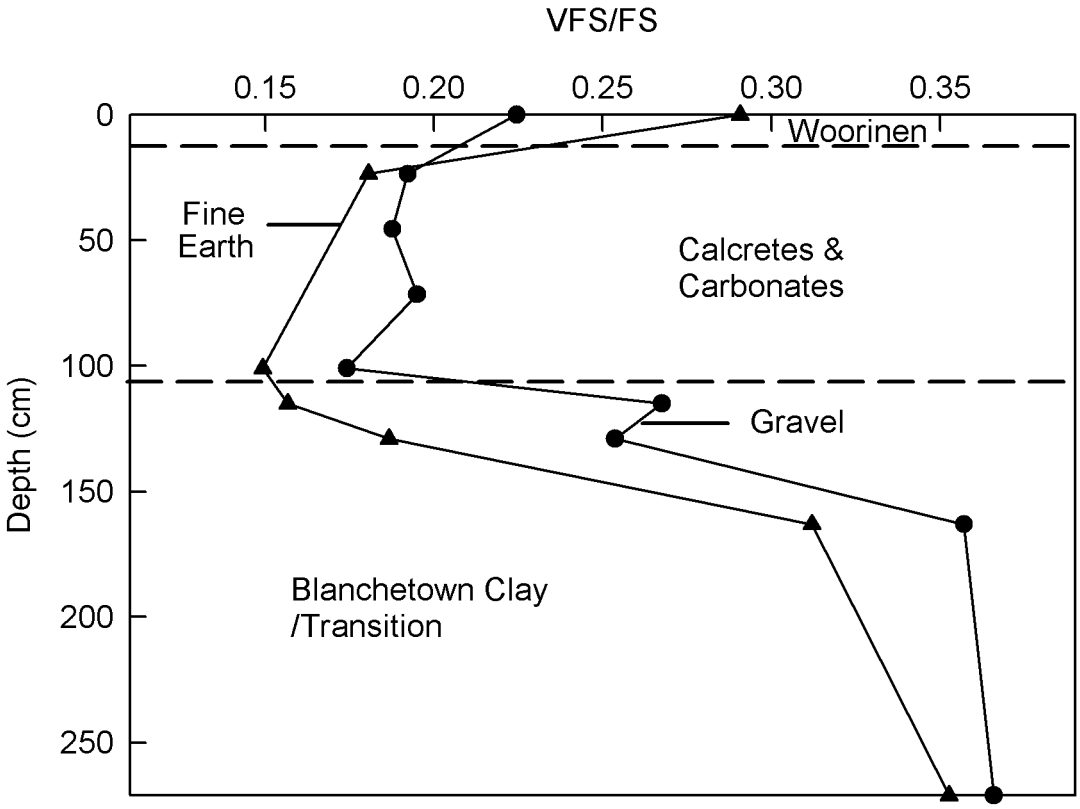
VFS/FS
0.15
0.20
0.25
0.30
0.35
0
50
100
150
200
250
Depth (cm)
Woorinen
Fine
Earth
Calcretes &
Carbonates
Gravel
Blanchetown Clay
/Transition

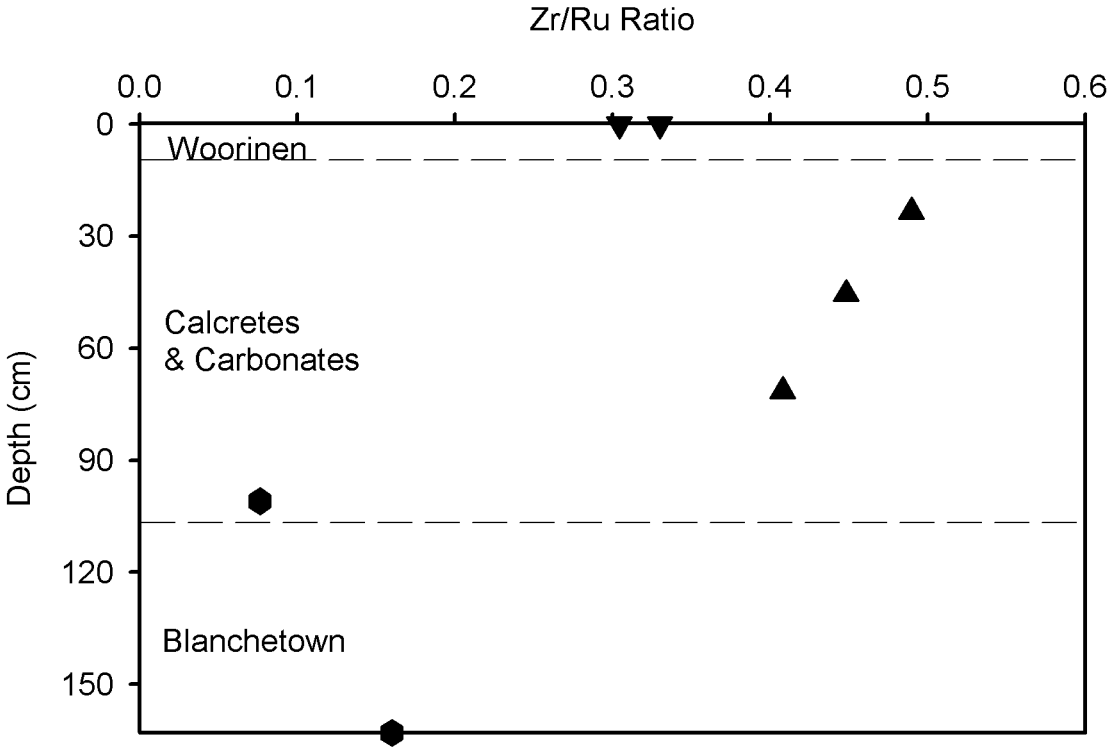
Zr/Ru Ratio
0.0
0.1
0.2
0.3
0.4
0.5
0.6
0
30
60
90
120
150
Depth (cm)
Woorinen
Calcretes
& Carbonates
Blanchetown

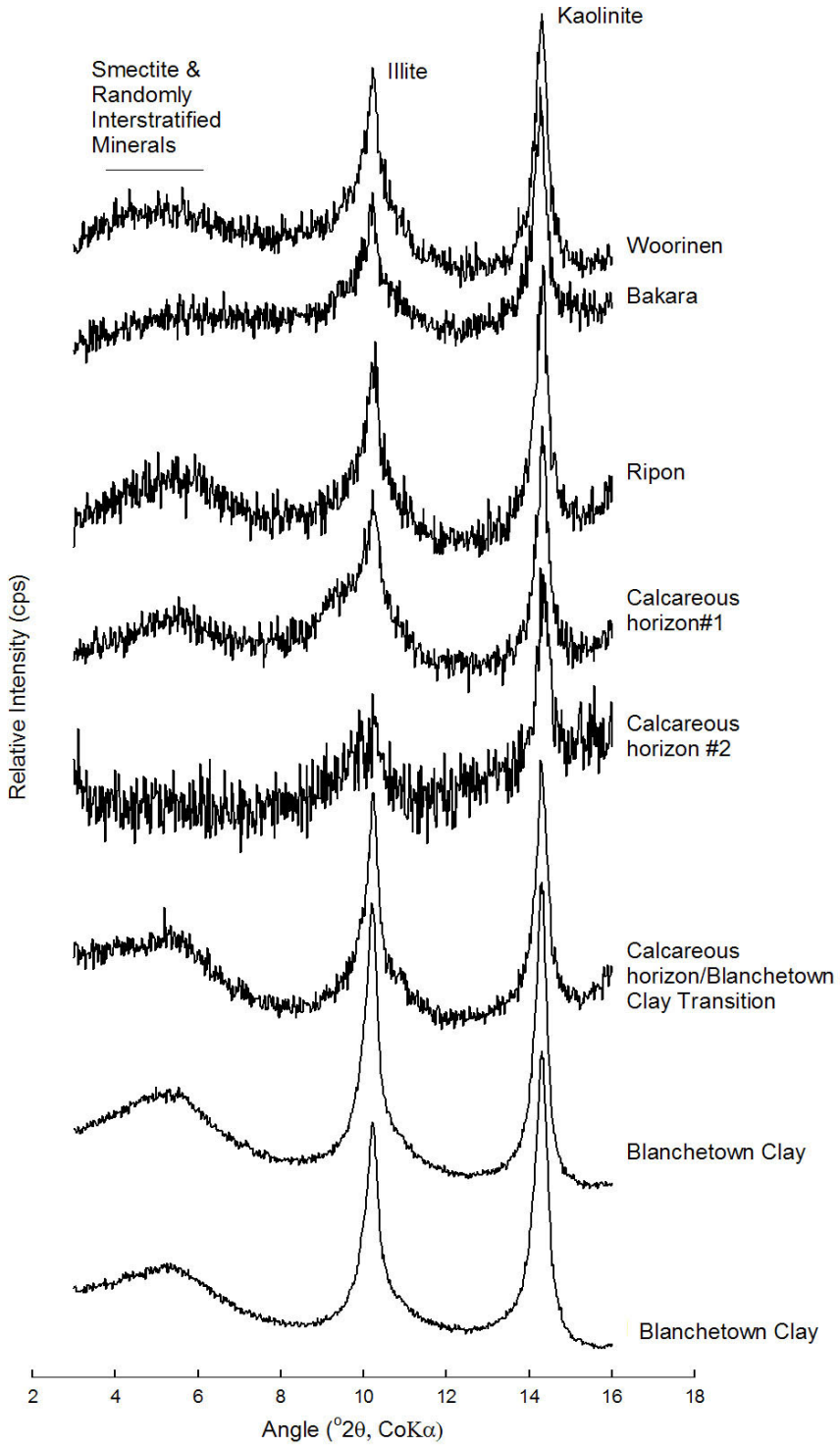
Kaolinite
Smectite &
Randomly
Interstratified
Minerals
Illite
Woorinen
Bakara
Ripon
Calcareous
horizon#1
Calcareous
horizon #2
Calcareous
horizon/Blanchetown
Clay Transition
Blanchetown Clay
Blanchetown Clay
Relative Intensity (cps)
2
4
6
8
10
12
14
16
18
Angle (°2θ, CoKα)

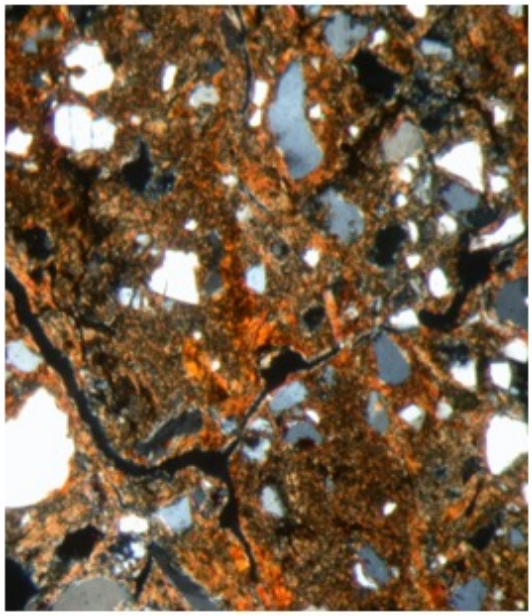

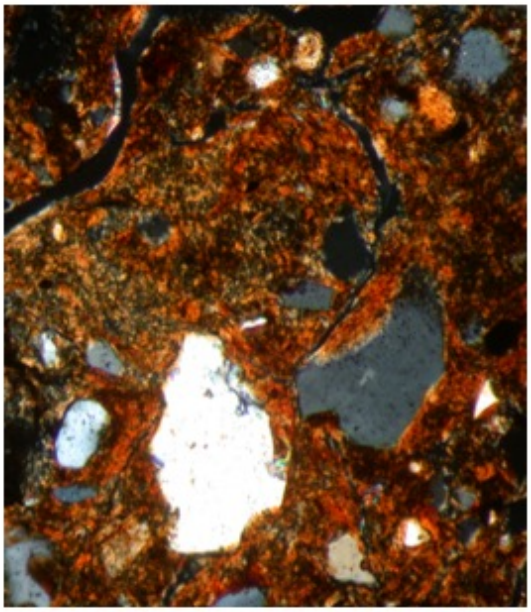

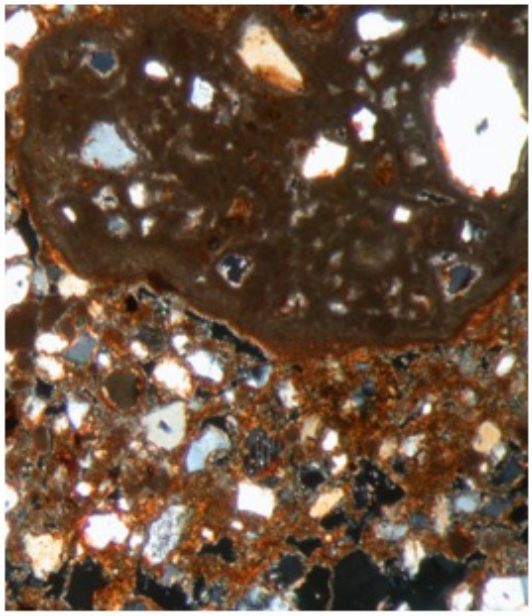

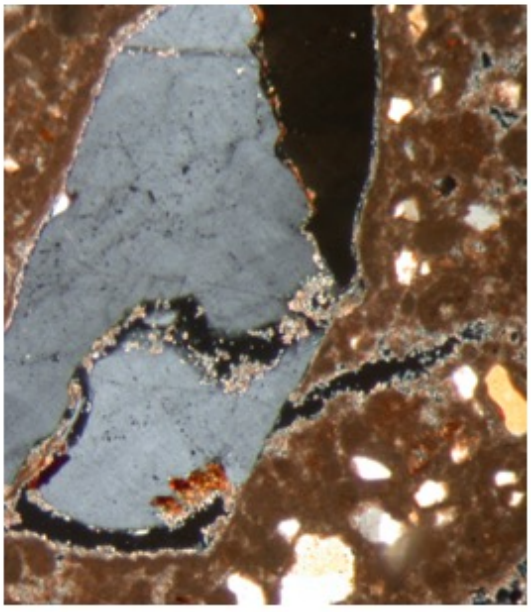

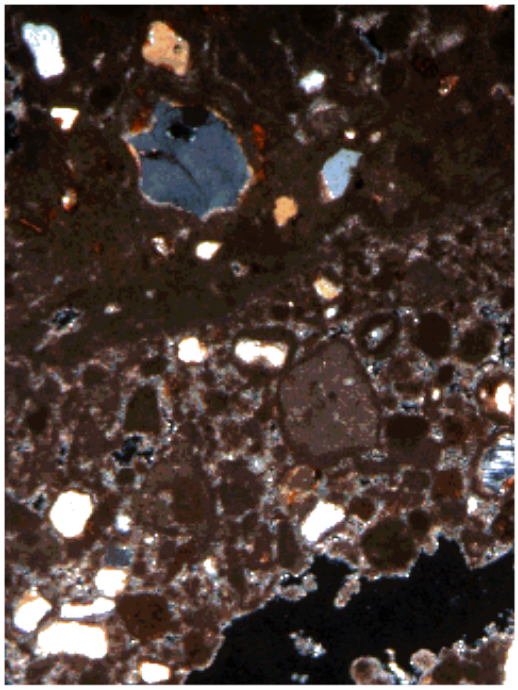

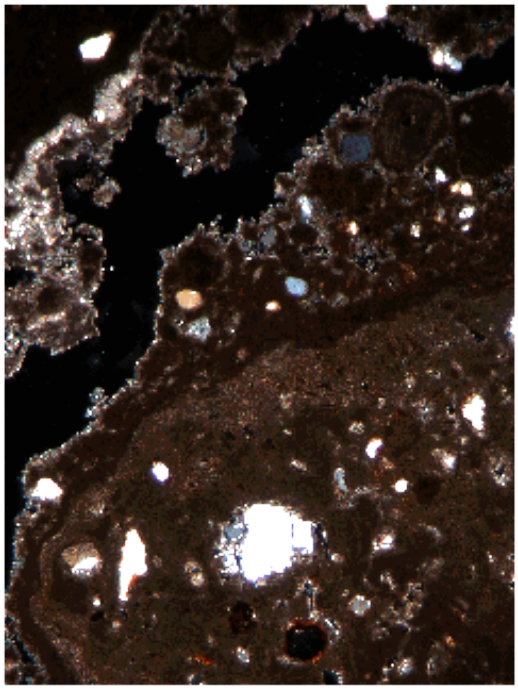

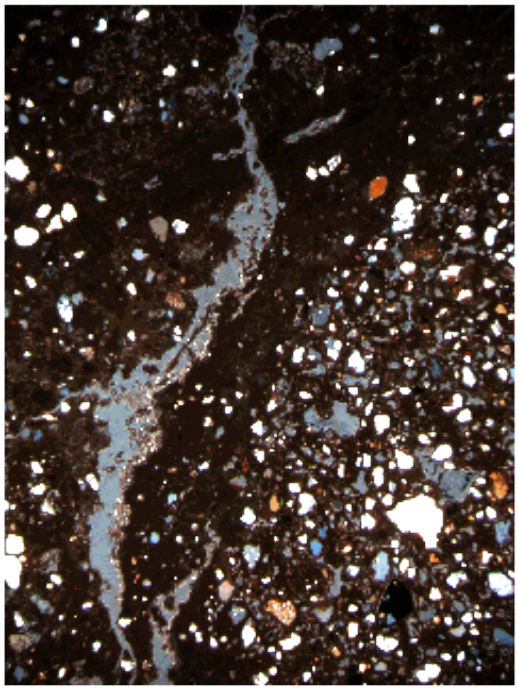

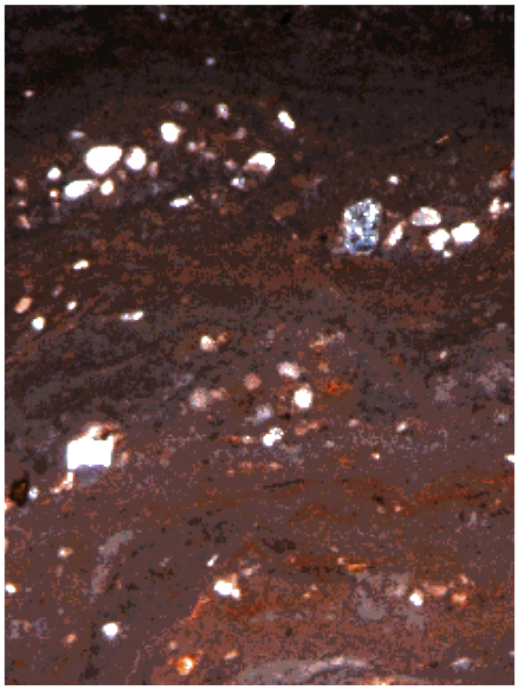

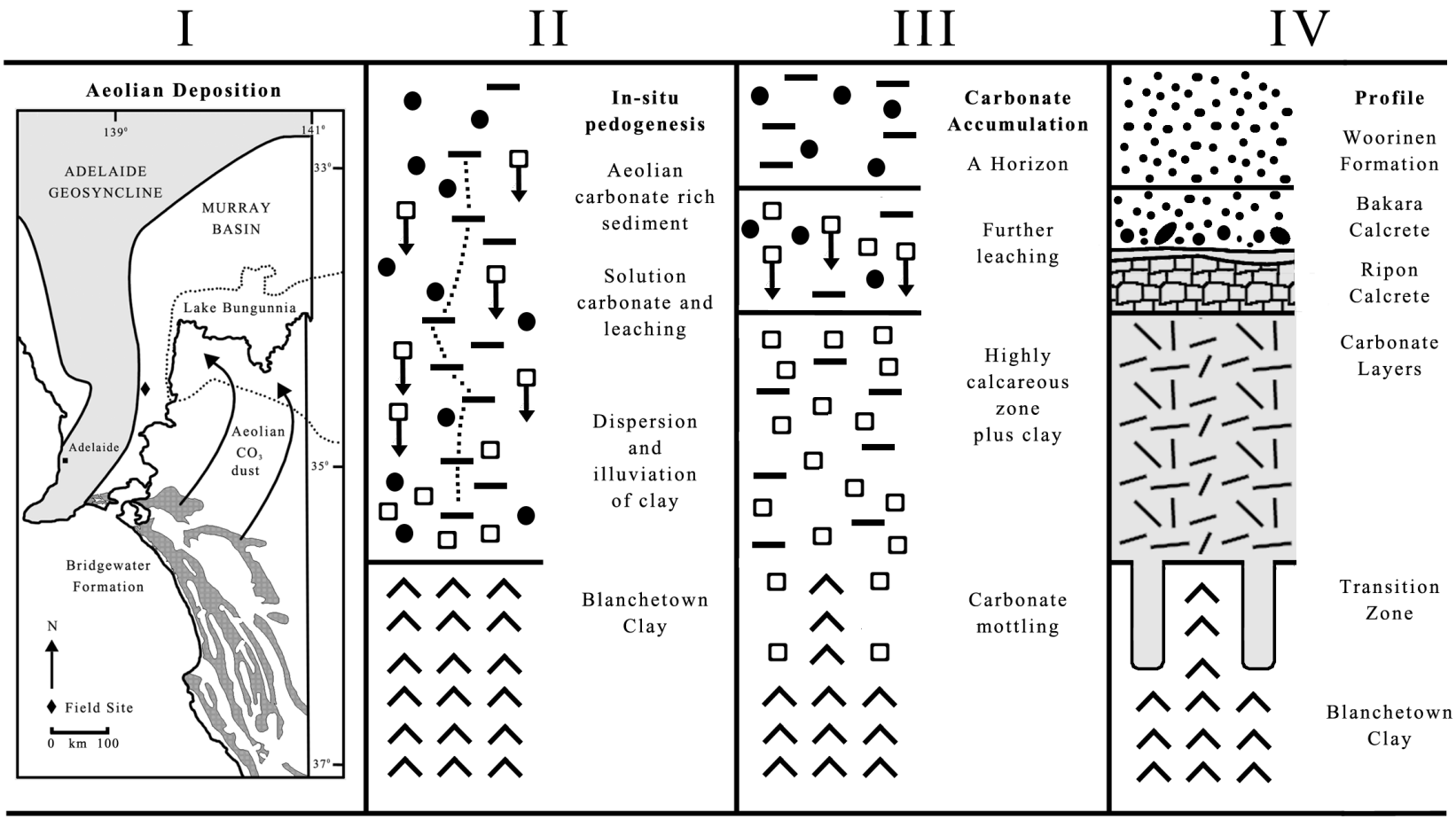
I
II
III
IV
Aeolian Deposition
139°
141°
33°
35°
37°
ADELAIDE
GEOSYNCLINE
MURRAY
BASIN
Lake Bungunnia
Adelaide
Aeolian
CO_3
dust
Bridgewater
Formation
N
Field Site
0 km 100
In-situ
pedogenesis
Aeolian
carbonate rich
sediment
Solution
carbonate and
leaching
Dispersion
and
illuviation
of clay
Blanchetown
Clay
Carbonate
Accumulation
A Horizon
Further
leaching
Highly
calcareous
zone
plus clay
Carbonate
mottling
Profile
Woorinen
Formation
Bakara
Calcrete
Ripon
Calcrete
Carbonate
Layers
Transition
Zone
Blanchetown
Clay

Table 1 Particle size distribution (PSD) and sand particle size distribution percentages (%)

Sample	Depth (cms)	Clay <2μm	Silt 2-20μm	Sand 20-2000μm	Very Fine Sand 20-53μm	Fine Sand 53-125μm	Coarse Sand 125-2000μm
9a	5.00	14.16	7.70	78.14	10.70	47.66	41.64
8a	23.50	9.24	7.43	83.33	9.26	48.14	42.60
7a	45.50	7.50	7.25	85.25	9.37	49.91	40.72
6a	71.50	11.43	9.39	79.17	6.93	35.52	57.55
5a	101.00	8.92	10.11	80.98	4.94	28.35	66.72
4a	115.00	11.04	7.98	80.97	10.65	39.83	49.52
3a	129.00	12.97	9.32	77.71	11.96	47.14	40.90
2a	163.00	42.76	9.96	47.28	13.74	38.50	47.76
1a	205.00	42.61	6.67	50.72	15.67	42.84	41.49
Sample	Depth (cms)	Clay <2μm	Silt 2-20μm	Sand 20-2000μm	Very Fine Sand 20-53μm	Fine Sand 53-125μm	Coarse Sand 125-2000μm
9b	5.00	14.87	8.54	76.59	13.92	47.88	38.20
8b	23.50	9.96	7.25	82.80	8.24	45.63	46.13
5b	101.00	7.31	6.63	86.06	4.74	31.72	63.55
4b	115.00	8.30	4.13	87.56	5.27	33.60	61.13
3b	129.00	9.19	5.65	85.16	7.23	38.71	54.06
2b	163.00	36.81	7.92	55.27	10.57	33.87	55.56
1b	205.00	39.66	5.64	54.69	13.84	39.27	46.89

Table 2 Mineral Percentage (%) of the heavy mineral (>2.90g/cm^3) fraction of the 20-53μm and 53-125μm fractions

#Sample	Depth (cm)	Stratigraphy	Mineral Percentage (%)							*Total Grains
			Al/Si	Fe-O	Ilm	Rut	Zr	Tit	^Other	
20-53μm fraction										
9a	5	Woorinen	48.7	16.7	15.0	7.8	2.6	0.0	8.8	1328
9b	5		55.8	15.9	8.8	6.8	2.1	0.0	10.6	339
8a	23.5	Bakara	36.4	21.0	17.9	8.2	4.0	0.8	11.6	1193
7a	45.5	Ripon	19.7	25.8	21.8	8.9	4.0	1.5	18.2	325
6a	71.5	Carbonate	42.9	22.0	15.2	6.2	2.5	2.4	8.6	787
5a	101		43.5	15.9	16.5	10.5	0.8	2.3	10.4	1119
2b	163	Blanchetown	29.3	19.0	10.8	10.1	1.6	0.9	28.4	744
53-125μm fraction										
9a	5	Woorinen	57.6	6.7	1.3	1.6	0.0	0.0	32.7	373
9b	5		56.1	8.4	1.3	2.4	0.0	0.0	31.6	538
8a	23.5	Bakara	84.7	6.4	3.3	1.3	0.4	0.1	3.9	1661
7a	45.5	Ripon	70.4	8.2	0.8	0.0	0.3	0.0	20.1	389
6a	71.5	Carbonate	76.7	12.6	2.4	1.4	0.3	0.0	6.7	1099
5a	101		61.0	21.9	4.4	0.8	0.1	0.2	11.5	1204
2b	163	Blanchetown	36.9	19.3	10.6	8.2	1.4	0.8	22.8	1383

* Total grains counts have been collected by a Philips XL30 field emission scanning electron (FESEM) microscope by setting the brightness and contrast to remove contamination by light minerals (<2.9g/cm^3) and setting the minimum diameter of grains at 5μm

^ Other minerals include contaminated minerals by W from the reagant, undifferentiated mineral assemblages, monazite, xenotime, alumia oxides and calcite

Samples labelled a are from the gravel fraction (>2mm) and samples labelled b are from the fine earth fraction (<2mm)

Appendix 1 Reagents used in organic carbon measurements

1N potassium dichromate ($K_2Cr_2O_7$)
0.5N ferrous sulphate ($FeSO_4.7H_2O$) containing 1.5% concentrated H_2SO_4
20mls concentrated H_2SO_4
200mls distilled H_20
10mls concentrated orthophosphoric acid
o-phenanthroline indicator

μ